

A functional m⁶A-RNA methylation pathway in the oyster *Crassostrea gigas* assumes epitranscriptomic regulation of lophotrochozoan development

Lorane Le Franc^{1,2}, Benoit Bernay³, Bruno Petton⁴, Marc Since⁵, Pascal Favrel^{1,2} and Guillaume Rivière^{1,2} 

1 UNICAEN, CNRS, BOREA, Normandie Univ, Caen, France

2 Laboratoire Biologie des organismes et Ecosystèmes aquatiques (BOREA), Muséum d'Histoire naturelle, CNRS, IRD, Sorbonne Université, Université de Caen Normandie, Université des Antilles, Caen, France

3 UNICAEN, ICORE, PROTEOGEN Core Facility, Caen, SF, France

4 Ifremer, Laboratoire des Sciences de l'Environnement Marin, UMR 6539 CNRS/UBO/IRD/Ifremer, Centre Bretagne, Normandie Univ, Plouzané, France

5 UNICAEN, Comprehensive Cancer Center F. Baclesse, SF ICORE, PRISMM Core Facility, Normandie Univ, Caen, France

Keywords

development; epitranscriptomics; methylation; oyster; RNA

Correspondence

G. Rivière, UNICAEN, CNRS, BOREA, Normandie Univ, 14000 Caen, France
Tel: +33231565113
E-mail: guillaume.riviere@unicaen.fr

(Received 7 February 2020, revised 13 June 2020, accepted 28 July 2020)

doi:10.1111/febs.15500

N⁶-methyladenosine (m⁶A) is a prevalent epitranscriptomic mark in eukaryotic RNA, with crucial roles for mammalian and ecdysozoan development. Indeed, m⁶A-RNA and the related protein machinery are important for splicing, translation, maternal-to-zygotic transition and cell differentiation. However, to date, the presence of an m⁶A-RNA pathway remains unknown in more distant animals, questioning the evolution and significance of the epitranscriptomic regulation. Therefore, we investigated the m⁶A-RNA pathway in the oyster *Crassostrea gigas*, a lophotrochozoan model whose development was demonstrated under strong epigenetic influence. Using mass spectrometry and dot blot assays, we demonstrated that m⁶A-RNA is actually present in the oyster and displays variations throughout early oyster development, with the lowest levels at the end of cleavage. In parallel, by *in silico* analyses, we were able to characterize at the molecular level a complete and conserved putative m⁶A machinery. The expression levels of the identified putative m⁶A writers, erasers and readers were strongly regulated across oyster development. Finally, RNA pull-down coupled to LC-MS/MS allowed us to prove the actual presence of readers able to bind m⁶A-RNA and exhibiting specific developmental patterns. Altogether, our results demonstrate the conservation of a complete m⁶A-RNA pathway in the oyster and strongly suggest its implication in early developmental processes including MZT. This first demonstration and characterization of an epitranscriptomic regulation in a lophotrochozoan model, potentially involved in the embryogenesis, bring new insights into our understanding of developmental epigenetic processes and their evolution.

Abbreviations

2/8 C, two- to eight-cell embryos; ALKBH5, AlkB homologue 5; B, blastula; CAN, acetonitrile; Cg-m⁶A-BPs, oyster m⁶A-interacting protein; D, D-larvae; E, oocytes; eIF3, eukaryotic initiation factor 3; F E, fertilized oocytes; FTO, fat mass and obesity-associated protein; G, gastrula; GO, Gene Ontology; HAKAI, RING finger E3 ubiquitin ligase; HNRNPA2B1, heterogeneous nuclear ribonucleoproteins A2/B1; hpf, hours postfertilization; M, morula; m⁶A, N⁶-methyladenosine; METTL, methyltransferase-like; MZT, maternal-to-zygotic transition; Prrc2a, proline-rich coiled-coil 2a; RBM15, RNA-binding motif 15; SAM, S-adenosyl-methionine; SPRI, solid-phase reversible immobilization; SSW, sterile sea water; TPM, transcripts per kilobase per million reads; WTAP, Wilms' tumour 1-associated protein; YTHDC, YTH domain-containing protein; YTHDF, YTH domain family protein; ZC3H13, zinc finger CCCH-type containing 13.

Introduction

The N⁶-methyladenosine (m⁶A) is the prevalent chemical RNA modification in all eukaryotic coding and non-coding RNAs [1]. Messenger RNAs are the most heavily m⁶A-methylated RNAs, with m⁶A bases lying mostly in their 3' UTRs, at the vicinity of their stop codon [2-4] and also in 5' UTRs and long internal exons [4,5]. N⁶ methylation of RNA adenosines is responsible for RNA processing and, like DNA methylation or histone modifications, contributes to the regulation of gene expression without changing the DNA or mRNA sequence. Therefore, m⁶A constitutes a new layer of post-transcriptional gene regulation, which is emerging or has been proven critical in various biological processes, and is referred to as epitranscriptomic [2].

The dynamics and biological outcomes of m⁶A levels are the results of the activity of a complex protein machinery comprising writers, erasers and readers. The addition of a methyl group to the 6th nitrogen of RNA adenosines is catalysed by m⁶A writers with distinct properties. Methyltransferase-like 16 (METTL16) is a 'stand-alone' class I methyltransferase that recognizes the UACA*GAGAA consensus sequence (with * indicating the target adenosine) [6]. By contrast, METTL3 transfers methyl groups to adenosines within the RRA*CH motif [2,3,7]. METTL3 is only active within a tripartite 'core complex' [8] comprising METTL3, METTL14 which enhances the methyltransferase activity supported by the MTA-70 domain of METTL3 [9,10] and the regulator protein Wilms' tumour 1-associated protein (WTAP) [4,9,11]. This core complex can interact with virilizer-like (or KIAA1429) [12], RING finger E3 ubiquitin ligase (HAKAI) [12,13], zinc finger CCCH-type containing 13 (ZC3H13) [12,14], RNA-binding motif 15 (RBM15) and RBM15B [7,15] which are suspected to intervene in the core complex activity and target specificity. The demethylation of adenosines has been demonstrated to be an active process catalysed by eraser enzymes belonging to the Fe(II)/2-oxoglutarate dioxygenase family: AlkB homologue 5 (ALKBH5) [16,17] and the fat mass and obesity-associated protein (FTO) [17,18].

A growing number of reader proteins which recognize the m⁶A-RNA mark are being described. They may be divided into two classes depending on the presence of a YT521-B homology (YTH) domain in their primary sequence. The YTH protein family includes YTH domain family protein 1-3 (YTHDF1-3) and YTH domain-containing protein 2 (YTHDC2), which are cytosolic m⁶A readers involved in m⁶A-RNA stability and translation [19-22]. The fifth YTH member is YTHDC1, which is present in the nucleus and controls

splicing [23] and nuclear export [24] of m⁶A-RNA. The second class of readers comprises proteins without YTH domain which are involved in several molecular mechanisms. For example, the heterogeneous nuclear ribonucleoprotein A2/B1 (HNRNPA2B1) is important for miRNA processing [25]. Insulin-like growth factor 2 mRNA-binding proteins 1-3 (IGF2BP1-3) [26] and proline-rich coiled-coil 2a (Prrc2a) [27] participate in RNA stability, while eukaryotic initiation factor 3 (eIF3) guides cap-independent translation [5].

The m⁶A epitranscriptomes underlie important biological functions, most of which being related to developmental processes, including the control of cell differentiation [27-32], maternal-to-zygotic transition (MZT) [33], sex determination [7,34] and gametogenesis [16,21,35,36]. Such critical epitranscriptomic outcomes are conserved in the animal evolution and were characterized in both vertebrates and ecdysozoans, that is mammals and drosophila.

However, such conserved biological significance originates in diverse epitranscriptomic mechanisms. Indeed, not all ecdysozoans bear a complete m⁶A-RNA machinery, such as *C. elegans* whose genome is devoid of the related protein machinery with the exception of a putative orthologue of METTL16 [37,38]. In addition, no m⁶A eraser has been described to date in nonvertebrate models, and especially ecdysozoans such as the drosophila or *C. elegans* [38-40], where it cannot be excluded that m⁶A-RNA methylation could be removed by the activity of characterized 6mA-DNA demethylases [41,42]. This situation may illustrate a growing complexity of epitranscriptomic mechanisms during the animal phylogeny and raises fundamental questions about its evolution and its presence in organisms distant from mammals and ecdysozoans. However, to date, no data about a possible epitranscriptomic regulation are available to our knowledge in lophotrochozoans, the understudied sister group of ecdysozoans within protostomes, although representing an important range of metazoan biodiversity.

The Pacific oyster *Crassostrea gigas* (i.e. *Magallana gigas*) is a bivalve mollusc whose great ecological and economical significance allowed its emergence as a model species within lophotrochozoan organisms. As such, an important amount of genetic, transcriptomic and epigenetic data has been generated in this model. Interestingly, the embryo-larval development of *C. gigas* is described to be under the strong epigenetic influence of DNA methylation [43-47] and histone marks [48-50]. Besides, oyster develop exposed to external environmental conditions, and in other models, the

m⁶A methylation of RNA and/or the expression of its machinery can be induced by heat stress, UV exposure or endocrine disruptors [5,51-54], questioning the presence of an m⁶A pathway in *C. gigas* and its significance in oyster early development.

To investigate this, we measured m⁶A levels in RNA across the entire embryo-larval life of the oyster using mass spectrometry and dot blot. We also searched the available *in silico* resources for putative conserved m⁶A-related proteins in *C. gigas* genomic data as well as their cognate expression kinetics using RNA-Seq assembly analyses. We also performed RNA pull-down with a synthetic m⁶A-RNA oligonucleotide coupled to liquid chromatography and mass spectrometry (LC-MS/MS) to characterize potential oyster m⁶A-binding proteins. To our knowledge, this study is the first report unravelling epitranscriptomic mechanisms outside vertebrate and ecdysozoan animal models.

Results

m⁶A is present in oyster RNA, differentially affects distinct RNA populations and displays variations during embryonic life

Mass spectrometry measurements revealed that m⁶A is present in oyster RNA, with global m⁶A/A levels of ca. 0.3%, a value comparable to what has been found in the human and the fruit fly (Fig. 1A). Immunoblot assays indicate that total and polyA + RNA present variable amounts of m⁶A during oyster development

and that these variations display distinct profiles suggesting specific methylation patterns between RNA populations. Indeed, m⁶A methylation in total RNA is the highest in the early stages (oocytes and fertilized oocytes) then gradually decreases until the morula stage before gradually increasing again up to the trochophore stage when it recovers its maximum (Fig. 1B). In contrast, m⁶A levels in polyA + RNA are hardly detected in early stages but display a peak in the gastrula and trochophore stages (Fig. 1C).

m⁶A machinery is conserved at the molecular level in the oyster

In silico analyses led to the identification of oyster sequences encoding putative orthologues of m⁶A writers, erasers and readers that are present in the human and/or in the human and the fruit fly.

All the eight m⁶A-RNA writers characterized in the human and/or drosophila at the time of the study, namely METTL3, METTL14, WTAP, virilizer-like, HAKAI, ZC3H13, RBM15/15B and METTL16, were present in the oyster at the gene level. The encoded protein primary sequences all display the specific domains required for enzymatic activity and/or binding. They include MT-A70 and AdoMetMtases SF domains for METTL3, METTL14 and METTL16, respectively, that bear the methyltransferase activity. Oyster WTAP and virilizer-like orthologues exhibit WTAP and VIR_N domains, respectively, that are required in their human counterparts to bind and

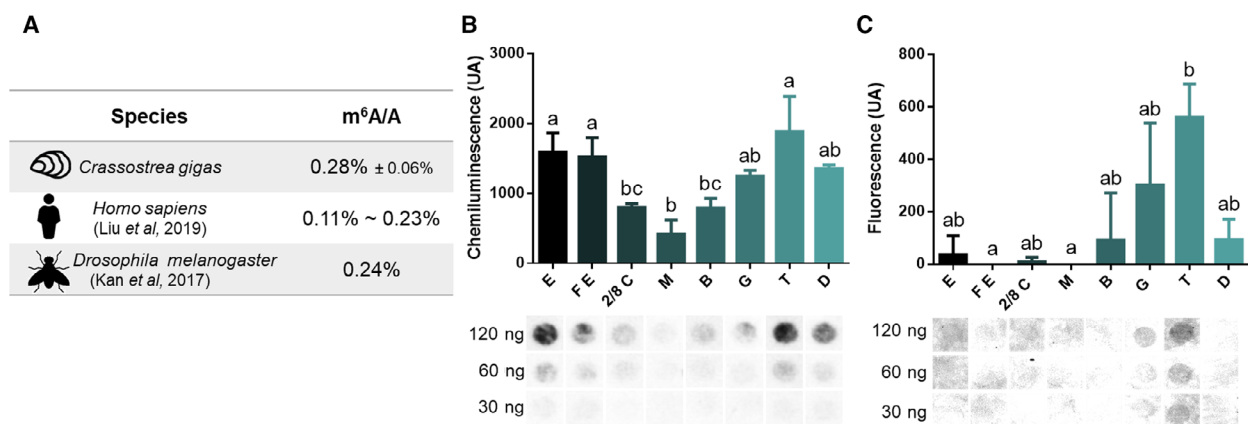


Fig. 1. m⁶A levels across oyster development. (A) m⁶A level quantified by LC-MS/MS in *Crassostrea gigas* embryo-larval stages pooled from oocytes to D-larvae ($n = 3$) is compared to the m⁶A level in *Homo sapiens* and *Drosophila melanogaster*; (B) dot blot quantification of m⁶A in total RNA throughout oyster development ($n = 3$); (C) dot blot quantification of m⁶A in polyA + RNAs throughout oyster development ($n = 3$), Kruskal–Wallis test, $\alpha < 0.05$. E, egg; F E, fertilized egg; 2/8 C, two- to eight-cell embryos; M, morula; B, blastula; G, gastrula; T, trochophore; D, D-larvae. Chemiluminescence (B) and fluorescence (C) are measured as a ratio between dot intensity of development stages and their respective controls for each amount of RNA (120, 60 and 30 ng). Data are presented as mean ± SD ($n = 3$).

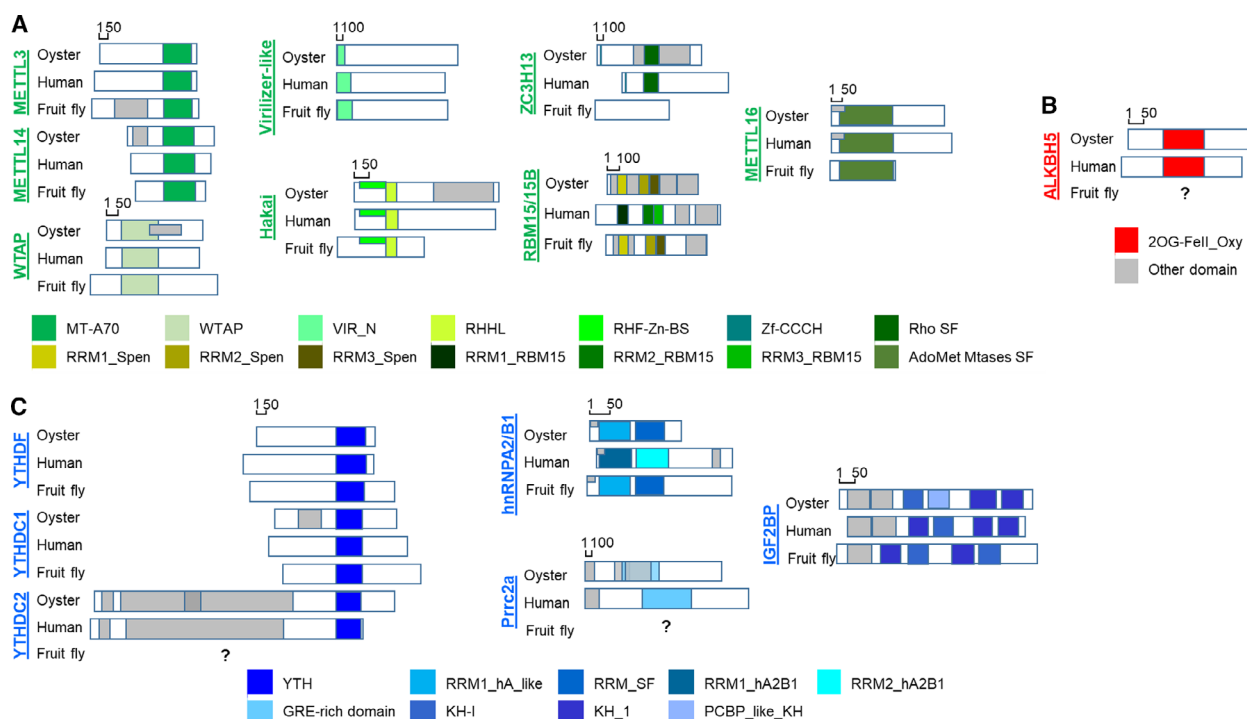


Fig. 2. The putative conserved m⁶A machinery in *Crassostrea gigas*. Domain architecture of actors of the m⁶A machinery identified by *in silico* analyses in the oyster compared to the fruit fly and human, (A) writer proteins; (B) eraser protein; (C) reader proteins. Putative domains involved in m⁶A processes are coloured (writers, green; eraser, red; readers, blue). Other domains identified but not involved in m⁶A processes are indicated in grey. Only one isoform is represented for each protein and each species for clarity (see Fig. S2 for other isoforms).

activate the catalytic subunit of the m⁶A-RNA methyltransferase complex. Oyster Hakai and RBM15/15B present RHH, RHF-Zn-BS and specific RRM domains, respectively, similar to human and fruit fly orthologues. Besides, the oyster ZC3H13 bears the Rho SF domain present in the human, but not in the fruit fly orthologue (Fig. 2A).

Crassostrea gigas also presents a putative m⁶A-RNA eraser, ALKBH5, which is present in the human but has not been characterized in drosophila. The oyster ALKBH5 exhibits a 2OG-FeII_Oxy domain suggestive of a presumably conserved catalytic functionality through Fe²⁺-dependent oxoglutarate oxidation. Of note, no orthologue of the human FTO eraser could be identified in the oyster genomic or transcriptomic databases available to date (Fig. 2B).

Many m⁶A reader orthologues have also been found in the oyster, including proteins containing a YTH domain, such as YTHDF, YTHDC1 and YTHDC2. An oyster Prrc2a-like protein produces homology with the human Prrc2a, especially within the m⁶A-binding GRE-rich domain. Oyster readers also include a heterogeneous nuclear ribonucleoprotein-coding gene,

hnRNPA2B1, with greater sequence similarity with the drosophila counterpart than with the human orthologue. Similarly, the IGF2BP-coding sequence has also been found in *C. gigas* (Fig. 2C). Five oyster sequences display homologies with eIF3a which is able to bind m⁶A-RNA [5], but it was not possible to discriminate whether a unique oyster predicted protein was an eIF3a orthologue.

Overall, these results indicate the conservation of a complete m⁶A-RNA machinery in the oyster. The complete list of the identified genes encoding the conserved m⁶A machinery actors and their isoforms, as well as the related information, is given in the Data S1.

Oyster putative m⁶A actors display expression level variations across development

RNA-Seq data analyses showed that all the oyster m⁶A-related genes were expressed during the early life (Fig. 3). Their expression level displayed gene-specific profiles, most of them being variable throughout oyster development.

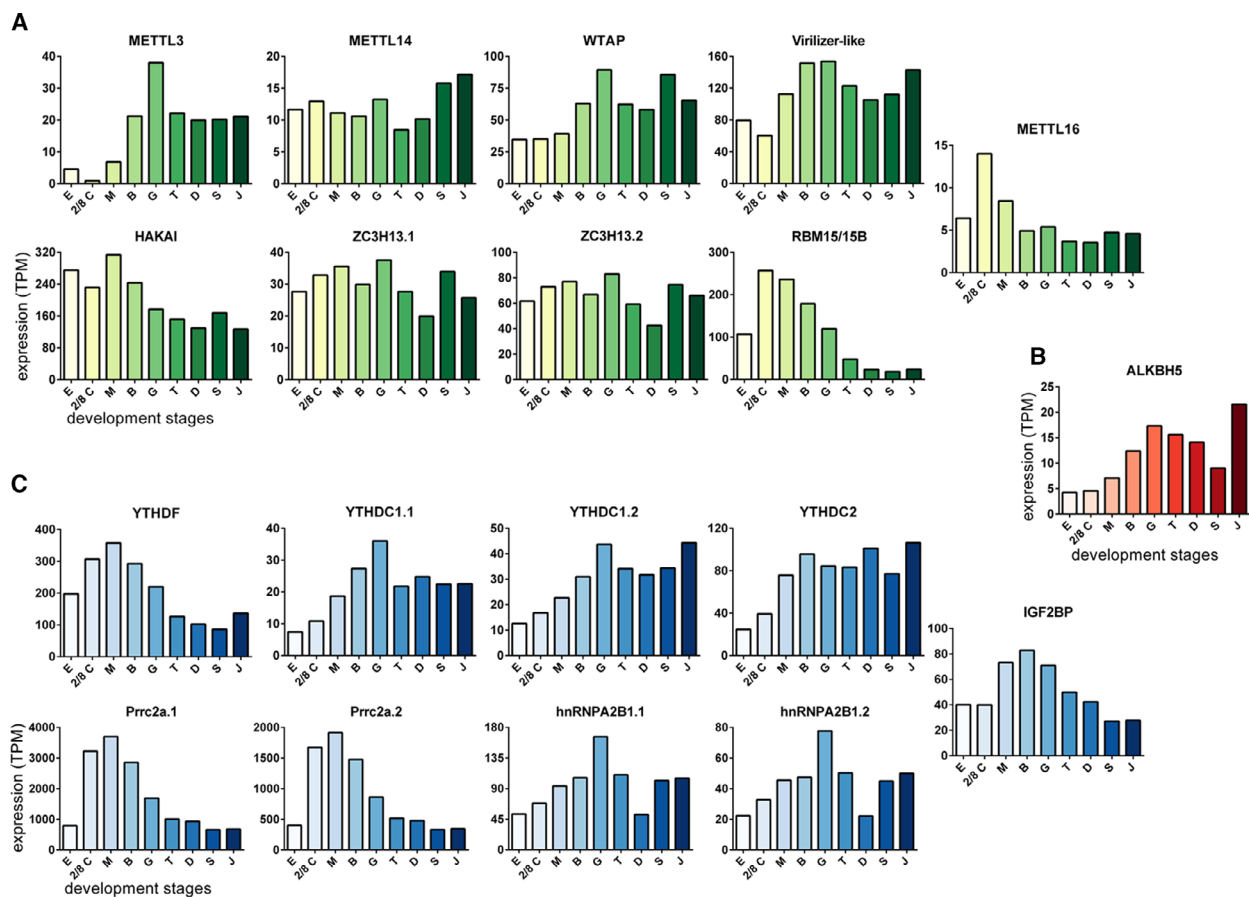


Fig. 3. Gene expression of the putative m⁶A machinery throughout oyster development. Expression levels of writers (A), eraser (B) and readers (C) identified by *in silico* analysis at each development stage were inferred from the GigaTON database. Expression levels are given in transcripts per kilobase per million reads (TPM) as the mean of the GigaTON values according to the Table S2. E, egg; 2/8C, two- to eight-cells; M, morula; B, blastula; G, gastrula; T, trochophore; D, D-larvae; S, spat; J, juvenile.

The expression of writers belonging to the core methylation complex is weak overall. METTL3 and WTAP share similar profiles with little expression increasing up to the gastrulation and remaining stable afterwards. In contrast, METTL14 displays a weak expression level across the embryo-larval life. The expression profile of virilizer-like resembles WTAP, while HAKAI, RBM15/15B and METTL16 seem to have mRNA levels which decrease after cleavage, whereas those of ZC3H13 transcript variants seem to drop at the D larva stage. Interestingly, METTL16 mRNA levels display an opposite developmental profile when compared to METTL3 expression, with the highest values during cleavage which decrease later on (Fig. 3A).

ALKBH5 transcripts are weakly represented within oyster early embryos, and the higher TPM values are found in gastrulas. However, maximum levels are observed after metamorphosis in juveniles (Fig. 3B).

Regarding m⁶A putative readers, the expression of YTH family genes during development showed different patterns. In fact, YTHDF is the most represented YTH domain-bearing actor and YTHDF TPM values are ca. fivefold higher than all the other oyster YTH readers. YTHDF is strongly expressed at the beginning of development until a peak at the morula stage. Prrc2a is the most represented reader at the mRNA level in oyster embryos, and the sum of the TPM of the two Prrc2a oyster isoforms is at most ca. 20-fold higher than that of YTH family. However, Prrc2a and YTHDF transcript content profiles are similar across oyster development and also remind of the IGF2BP mRNA levels.

By contrast, the two isoforms of YTHDC1 identified by *in silico* analysis, YTHDC1.1 and YTHDC1.2, display similar patterns together with YTHDC2, with a maximum representation in gastrulas. The

expression of hnRNPA2B1 isoforms has likewise patterns except for a marked drop at the D-larvae stage (Fig. 3C).

Oyster orthologues of m⁶A-RNA-interacting proteins bind m⁶A RNA *in vitro*

To determine whether oyster proteins can bind m⁶A-RNA, we performed RNA pull-down of cytoplasmic and nuclear embryonic cell extracts using a methylated versus a nonmethylated oligonucleotide, followed by LC/MS-MS characterization and identification of the captured proteins with the Mascot software.

In nuclear extracts, we detected 591 proteins able to bind both the methylated and unmethylated oligos. We identified 43 proteins specific to unmethylated RNA, while 131 proteins specifically bind the m⁶A-methylated oligo. In cytosolic extracts, there were 646, 436 and 36 of such proteins, respectively. Regardless of the methylation status, more proteins in the cytoplasmic extracts can bind to the RNA oligonucleotides than in the nuclear extracts (1118 vs. 765 proteins, respectively). However, more nuclear proteins are found exclusively bound to the m⁶A-containing oligo than cytoplasmic proteins (131 vs. 36, i.e. 17% vs. 3%, respectively). In addition, many nuclear and cytoplasmic proteins can bind both the methylated and the nonmethylated oligo (591 vs. 646, i.e. 77% vs. 58%). An important number of proteins in the cytoplasmic extract were found exclusively bound to the nonmethylated oligo, whereas only a limited number of nuclear proteins display such a specificity (436 vs. 43, i.e. 39% vs. 6%). Among the 167 m⁶A-specific proteins in oyster extracts, only 5 were found in both the nuclear and cytoplasmic extracts. These results show that oyster proteins can directly or indirectly bind m⁶A-RNA, and suggest an important compartmentalization of m⁶A-related processes.

Among the identified proteins in this assay, four of the putative oyster m⁶A readers are found, YTHDC1, hnRNPA2B1, IGF2BP and eIF3. In the nuclear extracts, YTHDC1 is uncovered as m⁶A-specific whereas hnRNPA2B1 and IGF2BP were present complexed with both the m⁶A- and A-oligos. In the cytoplasmic extracts, YTHDC1 and eIF3a are m⁶A-specific while hnRNPA2B1 and IGF2BP were pulled down by both methylated and unmethylated oligos (Fig. 4A).

These results demonstrate that some proteins in the oyster can specifically bind m⁶A-RNA and that the putative m⁶A reader orthologues in the oyster are conserved at the protein level and are able to interact with m⁶A-RNA.

The m⁶A-interacting protein-coding genes display clustered expression regulation and functional annotation during oyster development

The mRNA expression level of the genes encoding the 162 oyster m⁶A-interacting protein (Cg-m⁶A-BPs) was examined using RNA-Seq databases. Most of them display a specific and regulated expression level across oyster developmental stages. However, three main expression clusters could be distinguished according to their developmental mRNA expression level profile. Cluster 1 includes genes that show high expression at the beginning of the embryo life (i.e. cleavage) and strongly decrease after gastrulation; the cluster 2 contains weakly expressed genes except in the latest examined larval phases, after gastrulation (i.e. trochophore and D-larvae); and cluster 3 groups genes that show an expression peak during gastrulation (Fig. 4B).

The Gene Ontology annotation of the Cg-m⁶A-BP genes reveals that the distinct clusters are related to distinct functional pathways as indicated by the little—if any—common GO terms between them (Fig. 4C). However, the functional pathways of all three gene clusters point out to their implication in translation and its regulation, although the terms enriched in each cluster illustrate different aspects of translation, such as translation initiation (cluster 1), splicing and nuclear export (cluster 2) and ribosomal and mitochondrial processes (cluster 3), respectively (Fig. 4D).

Discussion

This work demonstrates that m⁶A-RNA is present and variable during the embryo-larval life of the oyster and that *C. gigas* exhibits putative conserved and functional m⁶A-RNA writers, eraser and readers. The dynamics of such mark and of its actors strongly suggest a biological significance of the epitranscriptomic pathway in the control of development of a lophotrochozoan species, which has, to date, never been demonstrated to our knowledge.

m⁶A-RNA levels vary across oyster development

Using mass spectrometry and immunological measurements, we showed that oyster RNA is m⁶A-methylated. The global proportion of N⁶-methyladenosine in RNA in the developing oyster (0.28%) is similar to those observed elsewhere in the animal kingdom, such as in the fruit fly (0.24%) [34] or the human (0.11–0.23%) [55] (Fig. 1A), despite those values are difficult to compare because they were not measured within the same developmental phase (adult flies and human cell

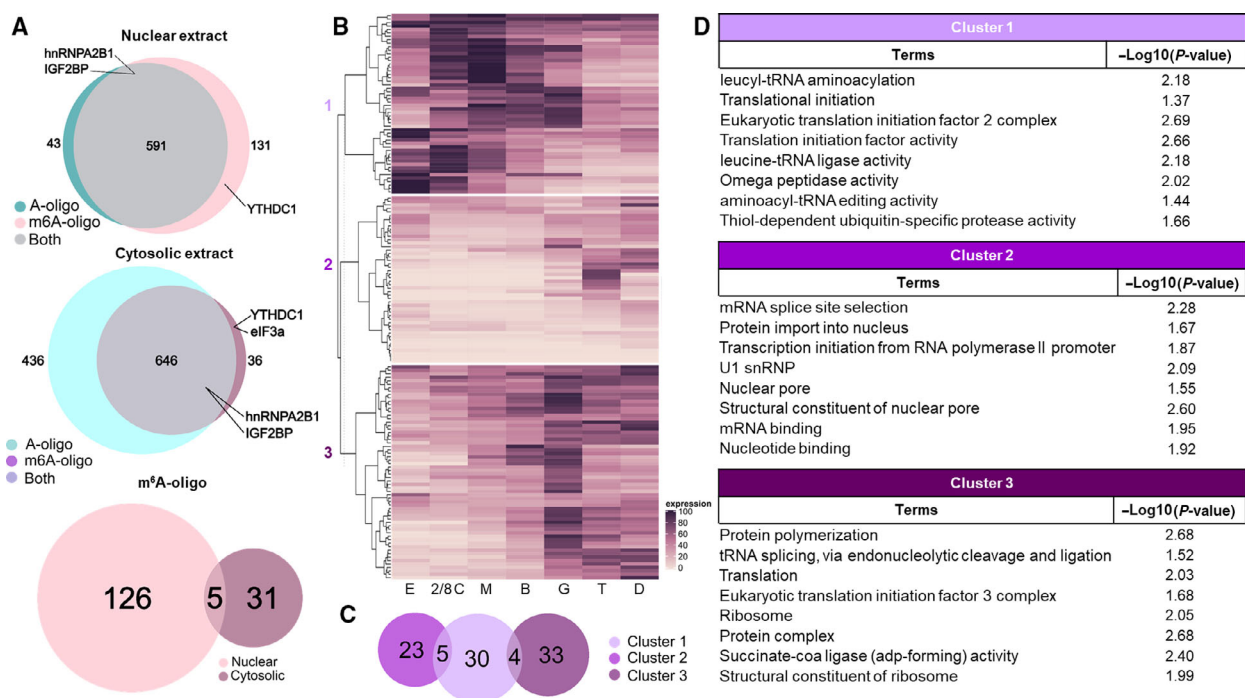


Fig. 4. Characterization of m⁶A-RNA-binding proteins in oyster development. (A) Venn diagram representation of proteins bound to the A- and/or m⁶A-oligos in nuclear and cytosolic fractions of oyster embryo-larval stages. The number of proteins identified is indicated. Some actors characterized in this study are highlighted: eIF3, YTHC1, hnRNPA2B1 and IGF2BP. (B) Heatmap of gene expression levels of the proteins that bind specifically to the m⁶A-oligo throughout oyster development. The expression level is normalized regarding the maximum value for each gene according to the GigaTON database. (C) GO term distribution among the three expression clusters in B. (D) Examples of GO term enrichment within the expression clusters of the m⁶A-bound proteins. The -log₁₀(P-value) associated with each term is given. E, egg; 2/8C: two- to eight-cells; M, morula; B, blastula; G, gastrula; T, trochophore; D, D-larvae; S, spat; J, juvenile.

lines vs. oyster embryos). However, the comparable magnitude of m⁶A-RNA amounts between taxa, in contrast to DNA methylation [46], may indicate conserved biological significance of epitranscriptomic processes between groups. The amount of m⁶A in total RNA displays a striking decrease during cleavage and then recovers its maximum levels at the end of the gastrulation (Fig. 1B). Therefore, the m⁶A decrease in total RNA during cleavage, that is before the transcription of the zygotic genome starts, reflects a degradation of maternal m⁶A-RNAs or their demethylation. However, all RNA populations do not exhibit the same pattern; indeed, polyA⁺ RNAs are m⁶A methylated only after cleavage. The extent of polyadenylation of oyster maternal messenger RNAs accumulating during vitellogenesis is unknown. Therefore, which maternal RNA population(s) is methylated in oyster oocytes is unclear. Nevertheless, the observation that m⁶A-RNA levels are variable and affecting distinct RNA populations across embryonic stages strongly favours an important biological significance of m⁶A-

RNA in oyster development. We hypothesize that oyster maternal messenger RNAs are poorly polyadenylated and that m⁶A, aside polyadenylation, might play a role in the stability of quiescent maternal mRNAs. Alternatively, other maternal RNA populations such as snRNA, miRNA, rRNA or lncRNA might be methylated [6,15,25,56], which become demethylated or degraded up to the morula stage. The later increase in m⁶A RNA after cleavage could therefore be the result of the methylation of the increasingly transcribed RNAs from the blastula stage, including polyadenylated mRNAs.

The m⁶A-RNA machinery is conserved in the oyster and regulated during development

The important regulation of m⁶A levels during oyster development assumes the presence of a related protein machinery. We identified *in silico* cDNA sequences encoding conserved putatively functional orthologues of m⁶A-RNA writers, eraser and readers in the oyster,

with great confidence (homologies ranging from ca. 30% to 65% with their human counterpart, see Data S1). The writers include all the members of the methylation complex (METTL3, METTL14, WTAP, virilizer-like, Hakai, ZC3H13, RBM15/15B) identified to date in the human and the fruit fly [7,8,11,12,14,15]. We also identified an orthologue of the stand-alone METTL16 m⁶A methyltransferase. Each orthologue bears the conserved domain(s) demonstrated to be implicated in the catalytic and/or binding activity of their cognate counterpart in other species, such as the MT-A70 domain which transfers methyl groups from the S-adenosyl-methionine (SAM) to the N⁶ nitrogen of RNA adenines [8]. Of the two proteins that can erase RNA methylation, only ALKBH5, which is important for mouse spermatogenesis [16], was identified at the cDNA level in the oyster. Indeed, no *C. gigas* sequence displayed significant homology with the mammalian FTO protein, whose functional significance remains controversial [17]. Most of the characterized m⁶A-RNA readers are also present at the molecular level in the oyster and are putatively able to bind m⁶A regarding their primary sequence, such as the YTHDC and YTHDF family members [19,21,23,57], Prrc2A [27], HnRNPA2B1 [25] and IGF2BP [26]. Of note, some of these readers have not been characterized to date in *D. melanogaster* but display strong homologies between humans and oysters. In mammals, eIF3a has important functional outcomes in cap-independent translational stress response [5]. However, it was not possible to ascribe a single oyster sequence as a unique eIF3a orthologue (Data S1), although its presence was demonstrated by RNA pull-down (see below) (see Data S2). Altogether, *in silico* results show the conservation of a complete m⁶A-RNA machinery in the oyster. To date to our knowledge, this is the first demonstration in a lophotrochozoan organism of an epitranscriptomic pathway. Its presence suggests its ancestral origin and questions its biological significance in oyster development.

To investigate this, we analysed the expression level of the m⁶A machinery genes using RNA-Seq data. Our results indicate that the core methylation complex (METTL3, METTL14 and WTAP) would not be active during cleavage because of the absence of METTL3 and little WTAP expression. METTL16 catalyses the downregulation of SAM methyl donor availability in mammals [58]. If METTL16 function is conserved in the oyster as suggested by the high sequence homology, the peak in METTL16 expression, together with the weak expression of the core complex in 2/8 cell embryos, is consistent with an absence of m⁶A-RNA up to the blastula stage. Then, the core

complex would likely be active as soon as the end of cleavage (i.e. since the blastula stage), in line with the increase in m⁶A levels observed at the same time. The correlation between the increasing METTL3 expression and m⁶A-RNA levels after cleavage strongly favours the conservation of the methyltransferase activity of the oyster MT-A70 domain. Interpreting the regulation of the m⁶A activity by the other methyltransferase complex members (i.e. virilizer-like, HAKAI, ZC3H13 and RBM15/15B) is difficult because how—or even if—oyster orthologues act within the complex is not known. Nevertheless, their specific expression profiles may reflect their implication in the regulation of distinct biological contexts. There might be little functional significance of active m⁶A-RNA erasure during oyster development, consistent with the normal embryonic phenotype of ALKBH5 knockdown mice [16]. Overall, the m⁶A readers display distinct developmental expression patterns. While YTHDF and Prrc2a peak during cleavage, YTHDC1, YTHDC2, IGF2BP and hnRNPA2B1 mRNA levels gradually increase up to the gastrulation and remain mostly highly expressed afterwards (except for hnRNPA2B1 and IGF2BP). These profiles evoke the mediation of distinct biological functions depending on the reader and the developmental phases. Therefore, we hypothesized that YTHDF and Prrc2a might participate in the blastulean transition in the oyster. Indeed, in the zebrafish, a YTHDF reader triggers the maternal-to-zygotic transition through the decay of the maternal m⁶A RNAs during cleavage [33]. The role in the axon myelination and specification of mouse oligodendrocytes [27] is unlikely conserved for Prrc2a because the oyster orthologue is expressed before the neurogenesis is detected in trochophore stages [59]. Alternatively, the early expression of Prrc2a suggests that it might rather compete with YTHDF for m⁶A-RNA targets [27], thereby possibly acting in oyster MZT, bringing new perspectives into this process which remains poorly understood in lophotrochozoans. In mammals, m⁶A is implicated in the embryonic cell fate [30,31] notably via the regulation of cell differentiation by YTHDC2 [32] or hnRNPA2B1 [29]. In the oyster, YTHDC1, YTHDC2, IGF2BP and hnRNPA2B1 have their maximum expression during gastrulation correlated to the second m⁶A peak, suggesting similar implications.

Putative oyster m⁶A readers actually bind m⁶A-RNA *in vitro*

To better approach the developmental processes involving m⁶A in the oyster, we characterized the

proteins that can interact with m⁶A-RNA using a methylated RNA pull-down/mass spectrometry assay. We identified 162 proteins able to specifically bind the m⁶A-RNA oligo in embryonic cell extracts, demonstrating the actual presence of genuine m⁶A readers in the oyster. Most (ca. 75%) of these proteins were found in nuclear extracts and only 5 were found in both the cytoplasmic and nuclear fractions, showing an important compartmentalization of the epitranscriptomic pathway. Regarding the little number of m⁶A readers in other animals, and because the assay conditions do not discriminate between direct and indirect interactions, we hypothesize that most of these proteins indirectly bind m⁶A via a limited number of 'scaffold' m⁶A readers. Such authentic readers that only bind the m⁶A-RNA oligo in our assay likely include YTHDC1 and eIF3a, which have been demonstrated to directly bind m⁶A in other species, demonstrating the conservation of the m⁶A-binding capacity and specificity of the YTH domain in the oyster. Besides, YTHDC1 is found in both cell fractions, suggesting its implication in the trafficking of m⁶A-RNA across the nuclear envelope [24], and reinforcing the hypothesis that YTH proteins could participate in oyster MZT and cell differentiation. The presence of the oyster eIF3a in the cytoplasm is consistent with a conserved role in m⁶A-mediated translation processes, such as cap-independent translation [5].

Possible functions of m⁶A-RNA in oyster development

We investigated the expression level and the functional annotation of the 162 genes encoding the m⁶A-interacting proteins across oyster early life. These genes can be clustered into three successive expression phases corresponding to three distinct functional pathways, which are independent albeit all mostly related to translation regulation. The cluster 1 is mostly expressed during the cleavage and the associated GO terms are related to the initiation of translation, consistent with maternal RNA consumption before MZT is complete and the zygotic genome becomes fully activated. The genes within cluster 3 show an expression peak during gastrulation. Their ontology terms evoke ribosomal and mitochondrial processes, the latter being required for energy supply and signalling integration during gastrulation [60-63]. The cluster 2 contains genes that peak after gastrulation and which are related to splicing and nuclear export. Such functional annotations are in line with a fine regulation of transcript variant translation within the distinct cell lineages in the three cell layers of the late embryos.

Taken together, our findings bring to light a possible implication of m⁶A in oyster development. First, during cleavage the decrease in m⁶A-RNA, the weak expression of methyltransferase complex genes, the maximum of YTHDF gene expression and the expression of Cg-m⁶A-BPs related to the initiation of the translation strongly suggest the implication of m⁶A in MZT in *C. gigas*. Second, the increasing m⁶A level during gastrula stage is correlated to the increase in methyltransferase complex gene expression. In addition, the increased RNA level of readers putatively related to cell differentiation and the peak of gene expression of Cg-m⁶A-BPs associated with ribosomal and mitochondrial processes support the hypothesis of a m⁶A implication in gastrulation. Finally, the highest m⁶A level at the trochophore stage, the gene expression of the methyltransferase complex and of readers associated with cell differentiation, as well as high RNA level of Cg-m⁶A-BPs related to splicing and nuclear export, are correlated with the fine cell differentiation taking place at this stage. However, inferring the biological significance of m⁶A in development from the indirect and incomplete functional annotation of the oyster genome is only limited. Characterization of the precise targets of m⁶A and how their individual methylation is regulated across development, for example, using high-throughput sequencing of precipitated m⁶A-RNA (MeRIP-seq), could be extremely relevant to better understand this issue. In addition, despite sequence conservation and binding ability of oyster actor orthologues strongly suggest functional conservation, future dedicated studies such as biochemical inhibition or gene inactivation could help demonstrate their genuine biological function. Besides, there seems to be an inverse correlation between m⁶A-RNA and 5mC-DNA levels during the considered oyster developmental window [46]. This may suggest an interplay between epigenetic and epitranscriptomic marks, possibly competing for methyl donor availability [58] or linked by histone epigenetic pathways [64,65].

Regarding the potential influence of the environment on m⁶A and the accumulation of RNA in oocytes, we are at present investigating our hypothesis that m⁶A may convey intergenerational epitranscriptomic inheritance of maternal life traits in the oyster. On an evolutionary perspective, the presence of a putatively fully conserved epitranscriptomic pathway in the oyster suggests that it was already present in the bilaterian common ancestor thereby favouring an important biological significance. Why *Drosophila* and *Caenorhabditis* seem to have lost specific m⁶A-RNA erasers could be related to a subfunctionalization of the DMAD [41] and NMAD-1 [42]. N⁶-methyladenine

DNA demethylase activity broadened towards RNA. However, more work is required to better understand the evo-devo implications of our results.

To conclude, in this work we report the discovery and characterization of a putatively complete epitranscriptomic pathway in a lophotrochozoan organism, the oyster *Crassostrea gigas*. This pathway includes the m⁶A mark in RNA and the actors of all the aspects of its regulation (writers, eraser and readers) which are conserved at the molecular level and putatively functional. We show that m⁶A levels are variable across oyster development and that m⁶A differentially affects distinct RNA populations. Expression levels of the related enzymatic machinery are consistent with the observed m⁶A level variations. We demonstrate the m⁶A binding capacity and specificity of putative oyster m⁶A readers in the cytoplasm and nucleus of embryolarval cells. These readers mediate distinct putative biological outcomes depending on the development stage considered. From these results, we hypothesize that early decay of maternal m⁶A RNA participates in maternal-to-zygotic transition during cleavage and that later *de novo* zygotic m⁶A methylation contributes to gastrulation and cell differentiation. This first characterization of an m⁶A-epitranscriptomic pathway in a lophotrochozoan organism, together with its potential implication in development, opens new perspectives on the evolution of epigenetic mechanisms and on the potential epitranscriptomic inheritance of environmentally induced life traits.

Methods

Animals

Broodstock oysters [66] and oyster embryos [46] were obtained at the IFREMER marine facilities (Argenton, France) as previously described. Briefly, gametes of mature broodstock oysters were obtained by stripping the gonads and filtering the recovered material on a 60- μ m mesh to remove large debris. Oocytes were collected as the remaining fraction on a 20- μ m mesh and spermatozoa as the passing fraction on a 20- μ m mesh. Oocytes were pre-incubated in 5 L of UV-treated and 1- μ m-filtered sterile sea water (SSW) at 21 °C until germinal vesicle breakdown. Fertilization was triggered by the addition of ca. 10 spermatozooids per oocyte. After the expulsion of the second polar body was assessed by light microscopy, embryos were transferred into 150-L tanks of oxygenated SSW at 21 °C. The development stages were determined by light microscopy observation. The stages collected were oocytes (E, immediately before sperm addition), fertilized oocytes (F E, immediately before transfer to 150-L tanks), two- to eight-cell embryos

(2/8C, ca. 1.5 h postfertilization (hpf)), morula (M, ca. 4 hpf), blastula (B, ca. 6 hpf), gastrula (G, ca. 10 hpf), trochophore (T, ca. 16 hpf) and D-larvae (D, ca. 24 hpf). For each development stage, 3 million embryos were collected as the remaining fraction on a 20- μ m mesh and centrifuged at 123 g for 5 min at room temperature. Supernatant was discarded, and samples of 1 million embryos were then snap-frozen in liquid nitrogen directly after resuspension in Tri-Reagent (Sigma-Aldrich, St Louis, MO, USA) (1 mL/10⁶ embryos) and stored at -80 °C. Three distinct experiments were realized (February to May 2019) using the gametes of 126 to 140 broodstock animals, respectively.

RNA extraction

Total RNA extraction

RNA was extracted using phenol-chloroform followed by affinity chromatography as previously described [67]. Briefly, embryos were ground in Tri-Reagent (Sigma-Aldrich) and RNA was purified using affinity chromatography (NucleoSpin RNA II Kit, Macherey-Nagel, Duren, Germany). Potential contaminating DNA was removed by digestion with rDNase (Macherey-Nagel) according to the manufacturer's instructions for 15 min at 37 °C; then, RNA was purified using Beckman Coulter's solid-phase reversible immobilization (SPRI) paramagnetic beads (Agencourt AMPure XP, Beckman Coulter, Brea, CA, USA) according to the manufacturer's instructions. Briefly, paramagnetic beads and RNAs were mixed slowly and incubated for 5 min at room temperature followed by 2 min on a magnetic rack. Cleared supernatant was removed, and beads were washed three times with 70% ethanol. After 4 min of drying at room temperature, RNAs were mixed slowly with RNase-free water and incubated for 1 min at room temperature on the magnetic rack. Eluted total RNA was stored at -80 °C.

PolyA RNA enrichment

PolyA RNA was extracted from total RNA by oligo-dT affinity chromatography (NucleoTrap mRNA Kit, Macherey-Nagel) according to the manufacturer's instructions. Briefly, up to 130 μ g of total RNAs was mixed with oligo-dT latex beads and incubated for 5 min at 68 °C then for 10 min at room temperature. After centrifugation (2000 g and then 11 000 g), the pellets were washed three times on the microfilter and dried by centrifugation at 11 000 g for 1 min. Finally, polyA + RNA was incubated with RNase-free water for 7 min at 68 °C then centrifuged at 11 000 g for 1 min. Eluted polyA + RNA was stored at -80 °C until needed.

Total and polyA-enriched RNA purity and concentrations were assayed by spectrophotometry (NanoDrop, Thermo Scientific, Waltham, MA, USA).

m⁶A quantification by LC-MS/MS

RNA hydrolysis

To generate nucleosides for quantification against standard curves, 5 µg of total RNA was denatured for 10 min at 70 °C followed by 10 min on ice and hydrolysed with 100 U nuclease S1 (50 U·µL⁻¹, Promega, Madison, WI, USA) in nuclease S1 buffer (Promega) in a final reaction volume of 25 µL for 2 h at 37 °C under gentle shaking. Samples were then incubated with alkaline phosphatase buffer (Promega) for 5 min at room temperature, before 10 U alkaline phosphatase (Promega) was added and incubated further for 2 h at 37 °C under gentle shaking. Ten extra units of alkaline phosphatase was added after 1 h of incubation to complete the reaction. Finally, samples were centrifuged at 20 000 g for 10 min at 4 °C, and the supernatant containing digested total RNA was collected and kept at -20 °C before quantification.

m⁶A quantification

The apparatus was composed of a NexeraX² UHPLC system coupled with LCMS-8030 Plus (Shimadzu, Kyoto, Japan) mass spectrometer using an electrospray interface in positive mode. The column (1.7 µm, 100 × 3 mm) was a HILIC ACQUITY[®] Amide (Waters, Milford, MA, USA) maintained at 35 °C. The injection volume and run-to-run time were 3 µL and 10 min, respectively. The flow rate was set to 1 mL·min⁻¹. Mobile phase was initially composed of a mixture of ammonium formate solution (10 mM) containing 0.2% (v/v) formic acid and 95% acetonitrile (ACN), and it was maintained for 1 min. Then, a linear gradient was applied to reach 83% ACN for 6 min. The composition returned to the initial conditions, and the column was equilibrated for 3 min.

The mass spectrometer was running in the multiple reaction monitoring (MRM) acquisition mode. LABSOLUTIONS 5.86 SP1 software (Shimadzu, Kyoto, Japan) was used to process the data. The desolvation temperature was 230 °C, source temperature was 400 °C, and nitrogen flows were 2.5 L·min⁻¹ for the cone and 15 L·min⁻¹ for the desolvation. The capillary voltage was +4.5 kV. For each compound, two transitions were monitored from the fragmentation of the [M + H]⁺ ion. The first transition (A in Table S1) was used for quantification and the second one (B in Table S1) for confirmation of the compound according to European Commission Decision 2002/657/EC (Table S1).

Blank plasma samples were analysed to check specificity. Calibrators were prepared using diluted solutions of A (Toronto Research Chemical, Toronto, Canada) and m⁶A (Carbosynth, Berkshire, UK) in water at 1, 2, 5, 10, 20, 50 and 100 ng·mL⁻¹. The calibration curves were drawn by plotting the ratio of the peak area of A and m⁶A. For both nucleosides, a quadratic regression with 1/C weighting

resulted in standard curves with $R^2 > 0.998$ and more than 75% of standards with back-calculated concentrations within 15% of their nominal values as recommended for by the European Medicines Agency for bioanalytical methods [68]. The limits of quantifications for both compounds were considered as the lowest concentrations of the calibration curve.

m⁶A/A ratios were calculated for each single sample using the determined concentrations. Final results are the average of three technical replicates.

m⁶A quantification by immunoblotting

Immunological quantification of m⁶A was performed by dot blot using total and polyA + RNAs. Dogfish total RNA (A. Gautier, personal communication) and a synthetic unmethylated RNA oligo (Eurogentec, Liege, Belgium) were used as positive and negative controls, respectively. RNA samples were denatured for 15 min at 55 °C with gentle shaking in denaturing solution (2.2 M formaldehyde, 50% formamide, 0.5X MOPS, DEPC water) followed by 2 min on ice. Blotting was performed on a vacuum manifold as follows: a nylon membrane (Amersham Hybond-N+, GE Healthcare life Sciences, Chicago, IL, USA) was prehydrated in DEPC water for 5 min; then, each well was washed twice with 10X SSC (Sigma-Aldrich) before RNA was spotted onto the membrane and incubated for 15 min at room temperature. Then, vacuum aspiration was applied and each well was washed twice with 10X SSC. After heat cross-linking for 2 h at 70 °C, the membrane was rehydrated with DEPC water for 5 min, washed with PBS and then PBST (PBS, 0.1% Tween-20) for 5 min each and blocked with two 5-min incubations with blocking buffer (PBS, 0.1% Tween-20, 10% dry milk, 1% BSA) at room temperature. The blocked membrane was incubated overnight at 4 °C under gentle shaking with the anti-m⁶A primary antibody (Total RNA: Millipore (Burlington, MA, USA) ABE572, 1: 1000 dilution in blocking buffer; polyA + RNA: Diagenode (Liege, Belgium) C15200082, 1: 500 dilution in blocking buffer) followed by four washes of PBST for 5 min. The secondary antibody (Total RNA: Dako (Santa Clara, CA, USA) P0447 goat anti-mouse HRP antibody, 1: 10 000 dilution; polyA + RNA: Invitrogen (Carlsbad, CA, USA) A21202 donkey anti-mouse Alexa 488, 1: 250 dilution) was diluted in PBST supplemented with 5% dry milk and added onto the membrane for 1 h 30 min (total RNA) or 1 h (polyA + RNA) at room temperature under gentle shaking. Membranes were extensively washed in PBST (at least 4 washes of 5 min for total RNA and 5 min and then 1 h for polyA + RNA); then, total and polyA + RNA immunoblots were visualized using chemiluminescence (ECL kit, Promega) or fluorescence scanning at 480–530 nm (ProXPRESS, PerkinElmer, Waltham, MA, USA), respectively. The amount of m⁶A was inferred from dot intensity

measurements using IMAGEJ (v.1.49) (<https://Imagej.net>). Signal intensities were determined as ‘integrated densities as a percentage of the total’ which corresponds to the area under the curve of the signal of each dot after membrane background and negative control signal subtraction.

***In silico* analyses**

All protein and RNA sequences of the m⁶A machinery of *Homo sapiens* and *Drosophila melanogaster* (Data S1) were recovered by their published designation (i.e. ‘METTL3’ or ‘YTHDF’) and their identified protein sequence (i.e. RefSeq accession number NP) collected from NCBI and used as query sequences to search for putative homologue sequences in *Crassostrea gigas* databases. The presence of oyster orthologue RNA and protein sequences was investigated by reciprocal BLAST (<https://blast.ncbi.nlm.nih.gov/Blast.cgi>) on the *Crassostrea gigas* GigaTON [69] and NCBI databases, and results were compared between the two oyster databases. Domain prediction was performed with CD search software (<https://www.ncbi.nlm.nih.gov/Structure/cdd/wrpsb.cgi>) with default settings on protein sequences of *Homo sapiens*, *Drosophila melanogaster* and *Crassostrea gigas*. The GRE-rich domain identified in vertebrate Prrc2a sequence [27] was performed with ProtParam (<https://web.expasy.org/protparam>).

Protein machinery mRNA expression analyses

The transcriptome data of the different development stages are available on the GigaTON database [69,70]. The correspondence between development stages in our study and the GigaTON database were assessed using light microscopy based on the morphological description by Zhang *et al.* [70] (Table S2). Expression data were expressed in TPM (transcripts per kilobase per million reads) [71] to provide a normalized comparison of gene expression between all samples. The actual presence of some transcripts that display unclear or chimeric sequences within available oyster databases was assessed using RT-PCR (Data S1).

Protein m⁶A RNA pull-down

Protein extraction and RNA affinity chromatography

Protein extraction and RNA affinity chromatography were performed as described previously [27] with some modifications as follows. Equal amounts (1 million individuals) of each developmental stage (oocyte to D-larvae) were pooled together then homogenized in 3.5 volumes of buffer A (10 mM KCl, 1.5 mM MgCl₂, 10 mM HEPES, pH 7.9, DEPC water, 1X protease inhibitor cocktail, DTT 0.5 mM) by extensive pipetting (ca. 30 times) and incubated for 10 min at 4 °C. Embryos were ground with 10 slow 23-G

needle syringe strokes and centrifuged at 500 g for 10 min at 4 °C. The supernatant was diluted in 0.11 volume of buffer B (1.4 M KCl, 0.03 M MgCl₂, HEPES 0.3 M, pH 7.9, DEPC water), centrifuged at 10 000 g for 1 h at 4 °C, and the supernatant containing cytosolic proteins was stored at –80 °C. The pellet of the first centrifugation, containing nuclei, was resuspended in two volumes of buffer C (0.42 M NaCl, 1.5 mM MgCl₂, 0.2 mM EDTA, 25% glycerol, 20 mM HEPES, pH 7.9, 0.5 mM PMSF, 0.5 mM DTT, water DEPC). Nuclei were then lysed with a 23-G needle (10 vigorous syringe strokes) followed by centrifugation at 25 000 g for 30 min at 4 °C, and the supernatant containing nuclear proteins was stored at –80 °C.

To identify putative proteins able to bind m⁶A-RNA, the cytosolic and nuclear fractions were submitted to affinity chromatography using 5'-biotin-labelled RNA oligonucleotides either bearing N⁶-methylated adenosines or not. The methylated adenosines were designed to lie within RRACH motifs, according to the conserved methylated consensus sequence in other organisms [2,3,7,33,72] (oligo-m⁶A: 5'Biotin-AGAAAAGACAACCAACGAGRR-m⁶A-CWCAUCAU-3'; oligo-A: 5'Biotin-AGAAAAGACAACCAACGAGRRACWCAUCAU-3', R = A or G, W = A or U, Eurogentec).

For RNA pull-down, streptavidin-conjugated magnetic beads (Dynabeads MyOne Streptavidin, Invitrogen) were preblocked with 0.2 mg·mL⁻¹ tRNA (Sigma-Aldrich) and 0.2 mg·mL⁻¹ BSA for 1 h at 4 °C under gentle rotation followed by three washes with 0.1 M NaCl. To avoid the identification of nontarget proteins, cytosolic and nuclear protein extracts were cleared with preblocked magnetic beads in binding buffer (50 mM Tris/HCl, 250 mM NaCl, 0.4 mM EDTA, 0.1% NP-40, DEPC water, 1 mM DTT, 0.4 U·μL⁻¹ RNasin) for 1 h at 4 °C under gentle rotation. After incubation on magnetic rack, the supernatants containing putative target proteins were collected and mixed with preblocked magnetic beads and oligo-m⁶A or oligo-A for 2 h at 4 °C under gentle rotation. The beads binding putative target proteins were washed three times with binding buffer and diluted in 50 mM ammonium bicarbonate.

Identification of m⁶A-binding proteins by LC-MS/MS

Protein samples were first reduced, alkylated and digested with trypsin then desalted and concentrated onto a μC18 Omix (Agilent, Santa Clara, CA, USA) before analysis.

The chromatography step was performed on a nanoElute (Bruker Daltonics, Billerica, MA, USA) ultra-high-pressure nanoflow chromatography system. Peptides were concentrated onto a C18 PepMap 100 (5 mm × 300 μm i.d.) precolumn (Thermo Scientific) and separated at 50 °C onto a reversed-phase Reprosil column (25 cm × 75 μm i.d.) packed with 1.6 μm C18-coated porous silica beads (Ionopticks, Parkville, Vic., Australia). Mobile phases consisted of 0.1% formic acid, 99.9% water (v/v) (A) and 0.1% formic

acid in 99.9% ACN (v/v) (B). The nanoflow rate was set at 400 nL·min⁻¹, and the gradient profile was as follows: from 2% to 15% B within 60 min, followed by an increase to 25% B within 30 min and further to 37% within 10 min, followed by a washing step at 95% B and re-equilibration.

MS experiments were carried out on an TIMS-TOF Pro mass spectrometer (Bruker Daltonics) with a modified nano-electrospray ion source (CaptiveSpray, Bruker Daltonics). The system was calibrated each week, and mass precision was better than 1 ppm. A 1600 spray voltage with a capillary temperature of 180 °C was typically employed for ionizing. MS spectra were acquired in the positive mode in the mass range from 100 to 1700 m/z. In the experiments described here, the mass spectrometer was operated in PASEF mode with exclusion of single-charged peptides. A number of 10 PASEF MS/MS scans were performed during 1.16 s from charge range 2–5.

The fragmentation pattern was used to determine the sequence of the peptide. Database searching was performed using the MASCOT 2.6.1 program (Matrix Science, London, UK) with a *Crassostrea gigas* UniProt database (including 25 982 entries). The variable modifications allowed were as follows: C-carbamidomethylation, K-acetylation, methionine oxidation and deamidation (NQ). The 'Trypsin' parameter was set to 'Semispecific'. Mass accuracy was set to 30 ppm and 0.05 Da for MS and MS/MS mode, respectively. Mascot data were then transferred to Proline validation software (<http://www.profi-proteomics.fr/proline/>) for data filtering according to a significance threshold of < 0.05 and the elimination of protein redundancy on the basis of proteins being evidenced by the same set or a subset of peptides (Data S2).

Gene ontology analysis

The mRNA sequences of the characterized m⁶A-binding proteins were identified using TBLASTN [73–75] against the GigaTON database [69] with default settings. Gene ontology (GO) analyses were carried out with the GO annotations obtained from GigaTON database gene universe [69]. GO term enrichment tests were performed using the GOSEQ (V1.22.0) R package [76] with *P*-values calculated by the Wallenius method and filtered using REVIGO [77]. GO terms with a *P*-value < 0.05 were considered significantly enriched (Data S3).

Statistical analyses and graph production

Results are given as the mean ± SD of three independent experiments unless otherwise stated. They were analysed using one-way ANOVA or Kruskal–Wallis tests when required, depending on the normality of result distribution. The normality was tested using the Shapiro–Wilk test and homoscedasticity of variances with Bartlett's tests. Statistics and graphics were computed with PRISM v.6 (GraphPad), R

(v.3.6.1) and RSTUDIO (v.1.0.153) softwares. The R packages *eulerr* [78] and *Complexheatmap* [79] were used for production of specific figures.

Acknowledgements

The authors would like to acknowledge PRISMM core facility collaborators R. Delepée and S. Lagadu for their expertise in m⁶A/A UHPLC-MS/MS quantification. We also thank J. Pontin for technical assistance and J. Le Grand for help with sampling. This work was supported by the French national programme CNRS EC2CO (Ecosphère Continentale et Côtière 'HERITAGE' to G. Rivière) and the Council of the Normandy Region (RIN ECUME to P. Favrel).

Conflict of interest

The authors declare no conflict of interest.

Author contributions

GR and LLF designed the experiment. LLF, GR, BB, BP and MS involved in benchwork and bioinformatics. LLF, GR, BB and MS analysed the data. LLF, GR, PF, BB, MS and BP wrote and edited the manuscript.

References

- Saletore Y, Meyer K, Korlach J, Vilfan ID, Jaffrey S & Mason CE (2012) The birth of the Epitranscriptome: deciphering the function of RNA modifications. *Genome Biol* **13**, 175.
- Meyer KD, Saletore Y, Zumbo P, Elemento O, Mason CE & Jaffrey SR (2012) Comprehensive analysis of mRNA methylation reveals enrichment in 3' UTRs and near stop codons. *Cell* **149**, 1635–1646.
- Dominissini D, Moshitch-moshkovitz S, Schwartz S, Salmon-Divon M, Ungar L, Osenberg S, Cesarkas K, Jacob-hirsch J, Amariglio N, Kupiec M *et al.* (2012) Topology of the human and mouse m⁶A RNA methylomes revealed by m⁶A-seq. *Nature* **485**, 201–206.
- Ke S, Alemu EA, Mertens C, Gantman EC, Fak JJ, Mele A, Haripal B, Zucker-Scharff I, Moore MJ, Park CY *et al.* (2015) A majority of m⁶A residues are in the last exons, allowing the potential for 3' UTR regulation. *Genes Dev* **29**, 2037–2053.
- Meyer KD, Patil DP, Zhou J, Zinoviev A, Skabkin MA, Elemento O, Pestova TV, Qian SB & Jaffrey SR (2015) 5' UTR m⁶A promotes cap-independent translation. *Cell* **163**, 999–1010.
- Pendleton KE, Chen B, Liu K, Hunter OV, Xie Y, Tu BP & Conrad NK (2017) The U6 snRNA m⁶A

- methyltransferase METTL16 regulates SAM synthetase intron retention. *Cell* **169**, 824–835.e14.
- 7 Lence T, Akhtar J, Bayer M, Schmid K, Spindler L, Ho CH, Kreim N, Andrade-Navarro MA, Poeck B, Helm M & *et al.* (2016) M6A modulates neuronal functions and sex determination in *Drosophila*. *Nature* **540**, 242–247.
 - 8 Bokar JA, Shambaugh ME, Polayes D, Matera AG & Rottman FM (1997) Purification and cDNA cloning of the AdoMet-binding subunit of the human mRNA (N6-adenosine)-methyltransferase. *RNA* **3**, 1233–1247.
 - 9 Liu J, Yue Y, Han D, Wang X, Fu YY, Zhang L, Jia G, Yu M, Lu Z, Deng X *et al.* (2013) A METTL3–METTL14 complex mediates mammalian nuclear RNA N6-adenosine methylation. *Nat Chem Biol* **10**, 93–95.
 - 10 Wang X, Feng J, Xue Y, Guan Z, Zhang D, Liu Z, Gong Z, Wang Q, Huang J, Tang C *et al.* (2016) Structural basis of N6-adenosine methylation by the METTL3–METTL14 complex. *Nature* **534**, 575–578.
 - 11 Ping X-LL, Sun B-FF, Wang L, Xiao W, Yang X, Wang W-JJ, Adhikari S, Shi Y, Lv Y, Chen Y-SS *et al.* (2014) Mammalian WTAP is a regulatory subunit of the RNA N6-methyladenosine methyltransferase. *Cell Res* **24**, 177–189.
 - 12 Yue Y, Liu J, Cui X, Cao J, Luo G, Zhang Z, Cheng T, Gao M, Shu X, Ma H *et al.* (2018) VIRMA mediates preferential m6A mRNA methylation in 3'UTR and near stop codon and associates with alternative polyadenylation. *Cell Discov* **4**, 10.
 - 13 Růžicka K, Zhang M, Campilho A, Bodi Z, Kashif M, Saleh M, Eeckhout D, El-Showk S, Li H, Zhong S *et al.* (2017) Identification of factors required for m6A mRNA methylation in *Arabidopsis* reveals a role for the conserved E3 ubiquitin ligase HAKAI. *New Phytol* **215**, 157–172.
 - 14 Knuckles P, Lence T, Haussmann IU, Jacob D, Kreim N, Carl SH, Masiello I, Hares T, Villaseñor R, Hess D *et al.* (2018) Zc3h13/Flacc is required for adenosine methylation by bridging the mRNA-binding factor Rbm15/Spenito to the m6A machinery component Wtap/Fl(2)d. *Genes Dev* **32**, 1–15.
 - 15 Patil DP, Chen CK, Pickering BF, Chow A, Jackson C, Guttman M & Jaffrey SR (2016) m6A RNA methylation promotes XIST-mediated transcriptional repression. *Nature* **537**, 369–373.
 - 16 Zheng G, Dahl JA, Niu Y, Fedorcsak P, Huang CM, Li CJ, Vågbo CB, Shi Y, Wang WL, Song SH *et al.* (2013) ALKBH5 is a mammalian RNA demethylase that impacts RNA metabolism and mouse fertility. *Mol Cell* **49**, 18–29.
 - 17 Mauer J, Luo X, Blanjoie A, Jiao X, Grozhik AV, Patil DP, Linder B, Pickering BF, Vasseur J-J, Chen Q *et al.* (2017) Reversible methylation of m6Am in the 5' cap controls mRNA stability. *Nature* **541**, 371–375.
 - 18 Jia G, Fu Y, Zhao X, Dai Q, Zheng G, Yang YGYY-GGYY-G, Yi C, Lindahl T, Pan T, Yang YGYY-GGYY-G & *et al.* (2011) N6-Methyladenosine in nuclear RNA is a major substrate of the obesity-associated FTO. *Nat Chem Biol* **7**, 885–887.
 - 19 Wang X, Lu Z, Gomez A, Hon GC, Yue Y, Han D, Fu Y, Parisien M, Dai Q, Jia G *et al.* (2014) N6-methyladenosine-dependent regulation of messenger RNA stability. *Nature* **505**, 117–120.
 - 20 Wang X, Zhao BS, Roundtree IA, Lu Z, Han D, Ma H, Weng X, Chen K, Shi H & He C (2015) N6-methyladenosine modulates messenger RNA translation efficiency. *Cell* **161**, 1388–1399.
 - 21 Hsu PJ, Zhu Y, Ma H, Guo Y, Shi X, Liu Y, Qi M, Lu Z, Shi H, Wang J *et al.* (2017) Ythdc2 is an N6-methyladenosine binding protein that regulates mammalian spermatogenesis. *Cell Res* **27**, 1115–1127.
 - 22 Shi H, Wang X, Lu Z, Zhao BS, Ma H, Hsu PJ, Liu C & He C (2017) YTHDF3 facilitates translation and decay of N6-methyladenosine-modified RNA. *Cell Res* **27**, 315–328.
 - 23 Xiao W, Adhikari S, Dahal U, Chen Y-S, Hao Y-J, Sun B-F, Sun H-Y, Li A, Ping X-L, Lai W-Y *et al.* (2016) Nuclear m6A reader YTHDC1 regulates mRNA splicing. *Mol Cell* **61**, 507–519.
 - 24 Roundtree IA, Luo G-ZZ, Zhang Z, Wang X, Zhou T, Cui Y, Sha J, Huang X, Guerrero L, Xie P *et al.* (2017) YTHDC1 mediates nuclear export of N6-methyladenosine methylated mRNAs. *eLife* **6**, 1–28.
 - 25 Alarcón CR, Goodarzi H, Lee H, Liu X, Tavazoie SFSSF & Tavazoie SFSSF (2015) HNRNPA2B1 is a mediator of m6A-dependent nuclear RNA processing events. *Cell* **162**, 1299–1308.
 - 26 Huang H, Weng H, Sun W, Qin X, Shi H, Wu H, Zhao BS, Mesquita A, Liu C, Yuan CL *et al.* (2018) Recognition of RNA N6-methyladenosine by IGF2BP proteins enhances mRNA stability and translation. *Nat Cell Biol* **20**, 285–295.
 - 27 Wu R, Li A, Sun B, Sun J-GG, Zhang J, Zhang T, Chen Y, Xiao Y, Gao Y, Zhang Q *et al.* (2018) A novel m6A reader Prrc2a controls oligodendroglial specification and myelination. *Cell Res* **29**, 23–41.
 - 28 Bertero A, Brown S, Madrigal P, Osnato A, Ortmann D, Yiangou L, Kadiwala J, Hubner NC, De Los Mozos IR, Sadee C *et al.* (2018) The SMAD2/3 interactome reveals that TGFβ controls m6A mRNA methylation in pluripotency. *Nature* **555**, 256–259.
 - 29 Kwon J, Jo YJ, Namgoong S & Kim NH (2019) Functional roles of hnRNPA2/B1 regulated by METTL3 in mammalian embryonic development. *Sci Rep* **9**, 8640.
 - 30 Geula S, Moshitch-Moshkovitz S, Dommissini D, Mansour AAF, Kol N, Salmon-Divon M, Hershkovitz V, Peer E, Mor N, Manor YS *et al.* (2015) m6A mRNA methylation facilitates resolution of naïve pluripotency toward differentiation. *Science* **347**, 1002–1006.

- 31 Batista PJ, Molinie B, Wang J, Qu K, Zhang J, Li L, Bouley DM, Lujan E, Haddad B, Daneshvar K *et al.* (2014) M⁶A RNA modification controls cell fate transition in mammalian embryonic stem cells. *Cell Stem Cell* **15**, 707–719.
- 32 Wojtas MN, Pandey RR, Mendel M, Homolka D, Sachidanandam R & Pillai RS (2017) Regulation of m⁶A transcripts by the 3'→5' RNA helicase YTHDC2 is essential for a successful meiotic program in the mammalian germline. *Mol Cell* **68**, 374–387.e12.
- 33 Zhao BS, Wang X, Beadell AV, Lu Z, Shi H, Kuuspalu A, Ho RK & He C (2017) M⁶A-dependent maternal mRNA clearance facilitates zebrafish maternal-to-zygotic transition. *Nature* **542**, 475–478.
- 34 Kan L, Grozhik AV, Vedanayagam J, Patil DP, Pang N, Lim K-S, Huang Y-C, Joseph B, Lin C-J, Despic V *et al.* (2017) The m⁶A pathway facilitates sex determination in *Drosophila*. *Nat Commun* **8**, 15737.
- 35 Kasowitz SD, Ma J, Anderson SJ, Leu NA, Xu Y, Gregory BD, Schultz RM & Wang PJ (2018) Nuclear m⁶A reader YTHDC1 regulates alternative polyadenylation and splicing during mouse oocyte development. *PLoS Genet* **14**, 1–28.
- 36 Ivanova I, Much C, Di Giacomo M, Azzi C, Morgan M, Moreira PN, Monahan J, Carrieri C, Enright AJ, O'Carroll D *et al.* (2017) The RNA m⁶A reader YTHDF2 is essential for the post-transcriptional regulation of the maternal transcriptome and oocyte competence. *Mol Cell* **67**, 1059–1067.e4.
- 37 Lence T, Paolantoni C, Worpenberg L & Roignant JY (2019) Mechanistic insights into m⁶A RNA enzymes. *Biochim Biophys Acta Gene Regul Mech* **1862**, 222–229.
- 38 Balacco DL & Soller M (2018) The m⁶A writer: rise of a machine for growing tasks. *Biochemistry* **58**, 363–378.
- 39 Lence T, Soller M & Roignant JY (2017) A fly view on the roles and mechanisms of the m⁶A mRNA modification and its players. *RNA Biol* **14**, 1232–1240.
- 40 Robbens S, Rouzé P, Cock JM, Spring J, Worden AZ & Van De Peer Y (2008) The FTO gene, implicated in human obesity, is found only in vertebrates and marine algae. *J Mol Evol* **66**, 80–84.
- 41 Zhang G, Huang H, Liu D, Cheng Y, Liu X, Zhang W, Yin R, Zhang D, Zhang P, Liu J *et al.* (2015) N⁶-methyladenine DNA modification in *Drosophila*. *Cell* **161**, 893–906.
- 42 Greer EL, Blanco MA, Gu L, Sendinc E, Liu J, Aristizábal-Corrales D, Hsu CH, Aravind L, He C & Shi Y (2015) DNA methylation on N⁶-adenine in *C. elegans*. *Cell* **161**, 868–878.
- 43 Riviere G, He Y, Tecchio S, Crowell E, Sourdain P, Guo X & Favrel P (2017) Dynamics of DNA methylomes underlie oyster development. *PLoS Genet* **13**, 1–16.
- 44 Sussarellu R, Lebreton M, Rouxel J, Akcha F, Riviere G & Rivière G (2018) Copper induces expression and methylation changes of early development genes in *Crassostrea gigas* embryos. *Aquat Toxicol* **196**, 70–78.
- 45 Rondon R, Grunau C, Fallet M, Charlemagne N, Sussarellu R, Chaparro C, Montagnani C, Mitta G, Bachère E, Akcha F & *et al.* (2017) Effects of a parental exposure to diuron on Pacific oyster spat methylome. *Environ Epigenet* **3**, 1–13.
- 46 Riviere G, Wu G-CC, Fellous A, Goux D, Sourdain P & Favrel P (2013) DNA methylation is crucial for the early development in the oyster *C. gigas*. *Mar Biotechnol* **15**, 1–15.
- 47 Saint-Carlier E & Riviere G (2015) Regulation of Hox orthologues in the oyster *Crassostrea gigas* evidences a functional role for promoter DNA methylation in an invertebrate. *FEBS Lett* **589**, 1459–1466.
- 48 Fellous A, Favrel P & Riviere G (2015) Temperature influences histone methylation and mRNA expression of the Jmj-C histone-demethylase orthologues during the early development of the oyster *Crassostrea gigas*. *Mar Genomics* **19**, 23–30.
- 49 Fellous A, Favrel P, Guo X & Riviere G (2014) The Jumonji gene family in *Crassostrea gigas* suggests evolutionary conservation of Jmj-C histone demethylases orthologues in the oyster gametogenesis and development. *Gene* **538**, 164–175.
- 50 Fellous A, Le Franc L, Jouaux A, Goux D, Favrel P & Rivière G (2019) Histone methylation participates in gene expression control during the early development of the Pacific Oyster *Crassostrea gigas*. *Genes (Basel)* **10**, 695.
- 51 Zhou J, Wan J, Gao X, Zhang X, Jaffrey SR & Qian S-B (2015) Dynamic m⁶A mRNA methylation directs translational control of heat shock response. *Nature* **526**, 591–594.
- 52 Lu Z, Ma Y, Li Q, Liu E, Jin M, Zhang L & Wei C (2019) The role of N⁶-methyladenosine RNA methylation in the heat stress response of sheep (*Ovis aries*). *Cell Stress Chaperones* **24**, 333–342.
- 53 Xiang Y, Laurent B, Hsu C, Nachtergaele S, Lu Z, Sheng W, Xu C, Chen H, Ouyang J, Wang S *et al.* (2017) m⁶A RNA methylation regulates the UV-induced DNA damage response. *Nature* **543**, 573–576.
- 54 Cayir A, Barrow TM, Guo L & Byun HM (2019) Exposure to environmental toxicants reduces global N⁶-methyladenosine RNA methylation and alters expression of RNA methylation modulator genes. *Environ Res* **175**, 228–234.
- 55 Liu J, Li K, Cai J, Zhang M, Zhang X, Xiong X, Meng H, Xu X, Huang Z, Fan J & *et al.* (2020) Landscape and regulation of M⁶A and M⁶Am methylome across human and mouse tissues. *Mol Cell* **77**, 426–440.
- 56 Ren W, Lu J, Huang M, Gao L, Li D, Greg Wang G & Song J (2019) Structure and regulation of ZCCHC4 in m⁶A-methylation of 28S rRNA. *Nat Commun* **10**, 5042.

- 57 Theler D, Dominguez C, Blatter M, Boudet J & Allain FHT (2014) Solution structure of the YTH domain in complex with N6-methyladenosine RNA: a reader of methylated RNA. *Nucleic Acids Res* **42**, 13911–13919.
- 58 Shima H, Matsumoto M, Ishigami Y, Ebina M, Muto A, Sato Y, Kumagai S, Ochiai K, Suzuki T & Igarashi K (2017) S-adenosylmethionine synthesis is regulated by selective N6-adenosine methylation and mRNA degradation involving METTL16 and YTHDC1. *Cell Rep* **21**, 3354–3363.
- 59 Yurchenko OV, Skiteva OI, Voronezhskaya EE & Dyachuk VA (2018) Nervous system development in the Pacific oyster, *Crassostrea gigas* (Mollusca : Bivalvia). *Front Zool* **15**, 1–21.
- 60 Ratnaparkhi A (2013) Signaling by folded gastrulation is modulated by mitochondrial fusion and fission. *J Cell Sci* **126**, 5369–5376.
- 61 Ren L, Zhang C, Tao L, Hao J, Tan K, Miao K, Yu Y, Sui L, Wu Z, Tian J & *et al.* (2017) High-resolution profiles of gene expression and DNA methylation highlight mitochondrial modifications during early embryonic development. *J Reprod Dev* **63**, 247–261.
- 62 Prudent J, Popgeorgiev N, Bonneau B, Thibaut J, Gadet R, Lopez J, Gonzalo P, Rimokh R, Manon S, Houart C *et al.* (2013) Bcl-wav and the mitochondrial calcium uniporter drive gastrula morphogenesis in zebrafish. *Nat Commun* **4**, 2330.
- 63 Dumollard R, Duchen M & Carroll J (2007) The role of mitochondrial function in the oocyte and embryo. *Curr Top Dev Biol* **77**, 21–49.
- 64 Huang H, Weng H, Zhou K, Wu T, Zhao BS, Sun MM, Chen Z, Deng X, Xiao G, Auer F *et al.* (2019) Histone H3 trimethylation at lysine 36 guides m⁶A RNA modification co-transcriptionally. *Nature* **567**, 414–419.
- 65 Wang Y, Li Y, Yue M, Wang J, Kumar S, Wechsler-Reya RJ, Zhang Z, Ogawa Y, Kellis M, Duester G & *et al.* (2018) N 6-methyladenosine RNA modification regulates embryonic neural stem cell self-renewal through histone modifications. *Nat Neurosci* **21**, 195–206.
- 66 Petton B, Pernet F, Robert R & Boudry P (2013) Temperature influence on pathogen transmission and subsequent mortalities in juvenile pacific oysters *Crassostrea gigas*. *Aquac Environ Interact* **3**, 257–273.
- 67 Riviere G, Fellous A, Franco A, Bernay B & Favrel P (2011) A crucial role in fertility for the oyster angiotensin-converting enzyme orthologue CgACE. *PLoS One* **6**, e27833.
- 68 EMA (2011) Guideline on bioanalytical method validation. EMEA/CHMP/EWP/192217/2009.
- 69 Riviere G, Klopp C, Ibouniyamine N, Huvet A, Boudry P & Favrel P (2015) GigaTON: an extensive publicly searchable database providing a new reference transcriptome in the pacific oyster *Crassostrea gigas*. *BMC Bioinformatics* **16**, 1–12.
- 70 Zhang G, Fang X, Guo X, Li L, Luo R, Xu F, Yang P, Zhang L, Wu F, Chen Y *et al.* (2012) The oyster genome reveals stress adaptation and complexity of shell formation. *Nature* **490**, 49–54.
- 71 Li B, Ruotti V, Stewart RM, Thomson JA & Dewey CN (2010) RNA-Seq gene expression estimation with read mapping uncertainty. *Bioinformatics* **26**, 493–500.
- 72 Qi ST, Ma JY, Wang ZB, Guo L, Hou Y & Sun QY (2016) N6 -methyladenosine sequencing highlights the involvement of mRNA methylation in oocyte meiotic maturation and embryo development by regulating translation in *Xenopus laevis*. *J Biol Chem* **291**, 23020–23026.
- 73 Altschul SF, Madden TL, Schäffer AA, Zhang J, Zhang Z, Miller W & Lipman DJ (1997) Gapped BLAST and PSI-BLAST: a new generation of protein database search programs. *Nucleic Acids Res* **25**, 3389–3402.
- 74 Cock PJA, Chilton JM, Grüning B, Johnson JE & Soranzo N (2015) NCBI BLAST+ integrated into Galaxy. *Gigascience* **4**, 39.
- 75 Camacho C, Coulouris G, Avagyan V, Ma N, Papadopoulos J, Bealer K & Madden TL (2009) BLAST+: architecture and applications. *BMC Bioinformatics* **10**, 1–9.
- 76 Young MD, Wakefield MJ, Smyth GK & Oshlack A (2010) Gene ontology analysis for RNA-seq: accounting for selection bias. *Genome Biol* **11**, R14.
- 77 Supek F, Bošnjak M, Škunca N & Šmuc T (2011) Revigo summarizes and visualizes long lists of gene ontology terms. *PLoS One* **6**, e21800.
- 78 Larsson J. (2019) eulerr: Area-Proportional Euler and Venn Diagrams with Ellipses. R package version 6.1.0. <https://cran.r-project.org/package=eulerr>
- 79 Gu Z, Eils R & Schlesner M (2016) Complex heatmaps reveal patterns and correlations in multidimensional genomic data. *Bioinformatics* **32**, 2847–2849.

Supporting information

Additional supporting information may be found online in the Supporting Information section at the end of the article.

Data S1. Complete list of *in silico* identified putative m⁶A machinery proteins and their respective BLAST results.

Data S2. Identified proteins by RNA pull down coupled with mass spectrometry with m⁶A or A-oligo, in nuclear or cytosolic protein extracts.

Data S3. Complete list of GO terms of clustered genes of m⁶A interacting proteins (p-value < 0.05).

Table S1. Transitions used for each compound. A: first transition, B: second transition.

Table S2. Table of correspondence between development stages in our study, and the GigaTON database.